Optimal Design of Self-Damped Lossy Transmission Lines in a Tree Network for Multichip Module

Jimmy S.-H. Wang and Wayne W.-M. Dai

UCSC-CRL-92-11
April 6,1992

Board of Studies in Computer Engineering
University of California, Santa Cruz
Santa Cruz, CA 95064

ABSTRACT

This paper addresses some of the problems encountered in propagating high-speed signals through lossy transmission lines on the substrates of silicon-on-silicon thin-film multichip modules (MCM). Instead of terminated by resistors, the lossy lines on the thin-film multichip modules can be structured to critically damp out the signal resonances, they are thus called *optimal, self-damped lossy transmission lines*. It is easiest to manufacture interconnection lines with fixed metal and dielectric thicknesses, and vary only the line width. This results in specific dependency of line width on length for self-damped lines. In this paper, we present a simple and robust method of designing self-damped lossy transmission lines in a tree network for multichip module. We vary the width of each branch of the network to meet certain electrical damping criteria. This results in stable operation as long as the lossy transmission line is shorter than the quarter wave length of the highest frequency component of interests. The lengths of lines on the silicon-on-silicon thin-film MCM substrate usually does not exceed this limit. If certain designs require larger substrate or higher speed, the materials and structural properties of the substrate (for example the dielectric thickness) is changed according to the method.

Keywords: transmission line, lossy, self-damped, critical damped, multichip module, multi-terminal network, distributed termination

1 Table of Contents

Contents

2 List of Tables and Figures

List of Figures

3 Introduction

The limiting factor for high performance systems is set by interconnection delay rather than by transistor switching speed. In high performance systems, 50 percent of the total system delay is usually contributed by packaging. This number may rise to 80 percent by the year 2000. As the operating frequency are pushed above 50 MHz, delay limited by the packaging technology becomes the pacing item for system clock speed.

While hybrid and Printed Circuit Board (PCB) have technical limitations in producing fine line geometries, thick-film methods and multilayer ceramic technologies yield high substrate permittivity. A new revolution in packaging technology called the multichip module (MCM) avoids many of the limitations of single chip packages. A multichip module has several bare chips mounted and interconnected on a substrate. By eliminating the individual chip packages, chips are placed closer together resulting in shorter interconnect lengths. Although multichip packaging is not new, the thin film multilayer interconnect technology allows a revolutionary advance in the performance of multichip packaging [BST87] [BMH89]. Compared to conventional packaging, MCM's can improve the system operating frequency by a factor of three, reduce area by a factor of seven, and reduce power consumption by 30% [Ohs89].

Multichip module packaging is used to design very high speed systems , and it uses less space than the conventional packaging techniques. By employing thin-film interconnect lines, the number of signal layers are reduced substantially (usually two signal layers with a power and a ground plane). The lines become lossy due to reduced dimensions, and behave differently from the *comparatively* lossless lines on a PC board [DKR+90]. The interconnect lines on thin-film substrate usually have the ohmic resistance that is comparable to the characteristic impedance. If a line is terminated with a load resistor of appropriate value to minimize signal reflections and resonances, the voltage divider formed by the termination resistance and the line characteristic impedance causes substantial and unacceptable attenuation of propagated signals. In addition, each termination dissipates quiescent power when the line is at non-zero voltage. This power drain negates the low-power-consumption advantage of CMOS circuitry [FT87].

This paper addresses the above mentioned problems encountered in propagating high-speed signals through lossy transmission lines, which are found on the silicon-on-silicon thin-film multichip modules. Instead of termination by resistors, the long lines on the thin-film multichip modules can be structured to critically damp the signal to avoid resonances. These lines are called *optimal self-damped lossy transmission lines* [FC91]. Since voltage doubling occurs at the end of the unterminated line due to reflection, a controlled amount of attenuation is tolerable. Being unterminated, the long lines in the substrate are structured to exhibit a total resistance that is related to the source resistance of the active devices which drives the lines. The relationship which determines the line resistance also depends on the characteristic impedance of the line, the resistivity of the interconnect material, the width and the thickness of the line, and the dielectric constant of the underlying dielectric material. The structured line which is critically damped can transmits input signal frequency components up to its resonance limit without any instability or attenuation. For higher frequencies, attenuation occurs but the line remains stable [HCBA82] [FT87] [FC91] [Bre91].

For high performance MCM systems, the interconnection lines are usually operating in the near transmission line regime. Due to the smaller cross section, the lines on MCM has a higher line resistance than a printed wiring board. Due to the longer line length, the lines on MCM has a higher line inductance than those used in very large scale integrated circuit. In order to properly analyze the response of the interconnections of multichip modules at all frequencies of interest, we must take into account the effects of both inductance and resistance [FT87].

In the following section, we will first analyze the point-to-point lossy transmission-line interconnection that determines the minimum loss needed to obtain a stable yet fast signal propagation in unterminated lines. For any particular driver impedance, there is a maximum length for critically damped interconnect lines. A longer line will become overdamped and hence slower than necessary. For a maximum length interconnect line on the substrate, it is feasible to determine a set of structural parameters required to achieve optimal high-speed operation of the line. Since it is easiest to manufacture interconnection lines with fixed metal and dielectric thicknesses, usually we vary only the line width. The width of a self-damped interconnect line is selectively proportioned as a function of its length. The width of shorter-than-maximum-length interconnect lines are narrowed relative to the width of the maximum-length interconnect line. Lines below a certain minimum length need not be structured [HCBA82].

We then extend the design method from point-to-point nets to multi-terminal nets. We introduce a technique to decompose the multi-terminal tree network into point-to-point segments to which we can apply the previous analysis. With this design method, optimal self-damped lossy transmission can be applied to all tree topology networks with a single driving source for multichip modules. The key parameter that ties everything together is the characteristic impedance of the interconnects. By controlling the characteristic impedance, we can maintain distortion-free propagation of high-speed signals and to control the ringing.

The limitations of this design method are detailed in the concluding section. The method results in stable operation as long as the highest frequency component of interesting transmitted by the lines does not exceed the frequency which corresponds to that the line length becomes the quarter-wave length. This is usually the case for most of the lines on the silicon-on-silicon thin-film MCM substrates. However, if some particular designs require larger substrate or higher speed, the materials and structural properties of the substrate (for example the dielectric thickness) can be changed to meet the requirement.

In conclusion, we have found an optimal design method for the design of high speed interconnection for MCM. This method uses an analytic formula to find the optimal width and characteristic impedance of each branch in tree networks.

4 Optimal Design of Self-Damped Lossy Transmission Line for Point-To-Point Net

In this section, we analyze embedded microstrip lines using Quasi-TEM assumptions. The detailed derivation of electromagnetic wave propagation can be found in the standard microwave textbooks [Lia87]. The parameters that characterize the lines are its per unit length inductance L, capacitance C, and resistance R. Here we assume the loss in the dielectrical layer is insignificant for typical multichip module substrates. Figure 4.1 shows the physical structure of a typical multichip module interconnections.

In the following, we summarize the analysis performed by Fry and Tai for point-to-point connection [FT87]. Let $V(z,t)$ represents the voltage on the interconnection line at point z distance from the driver at time t, and $I(z,t)$ represents the current on the interconnection

Figure 4.1: **Typica**

tions. It shows tw

Separating Equation (4.7) into its real and imaginary parts, and compare to 4 we have

$$\alpha = Re[\gamma] = \frac{R}{2}\sqrt{\frac{2C}{L}}\frac{1}{\sqrt{1+\sqrt{1+\frac{R^2}{\omega^2L^2}}}} = \frac{R}{2}\sqrt{\frac{2C}{L}}\frac{1}{\sqrt{1+\sqrt{1+\frac{\omega_c^2}{\omega^2}}}} \tag{4.8}$$

and

$$\beta = Im[\gamma] = \omega\sqrt{\frac{LC}{2}}\sqrt{1+\sqrt{1+\frac{R^2}{\omega^2L^2}}} = \omega\sqrt{\frac{LC}{2}}\sqrt{1+\sqrt{1+\frac{\omega_c^2}{\omega^2}}}. \tag{4.9}$$

Where in Equations (4.8) and (4.9), we have defined the critical frequency

$$\omega_c \equiv 2\pi f_c = \frac{R}{L}.$$

The parameter β is related to the phase velocity ν_p through

$$\nu_p = \frac{\omega}{\beta} = \frac{1}{\sqrt{LC}}\frac{\sqrt{2}}{\sqrt{1+\sqrt{1+\frac{\omega_c^2}{\omega^2}}}}. \tag{4.10}$$

At high frequencies, $\omega \gg \omega_c$, this expression simplifies to the well known result for lossless lines, $\nu_p = \frac{1}{\sqrt{LC}}$. The parameter α characterizes the attenuation on the line. Its expression simplifies to $\alpha = \frac{R}{2}\sqrt{\frac{C}{L}}$ at high frequencies. For all frequencies, R is equal to zero for a lossless line, in such case α is identically zero.

If we substitute Equations (4.5), (4.6), and (4.7) back into the Telegraphist's Equations (4.1) and (4.2), we have

$$I_+ = V_+\sqrt{\frac{j\omega C}{R+j\omega L}} \equiv \frac{V_+}{Z_0} \tag{4.11}$$

$$I_- = -V_-\sqrt{\frac{j\omega C}{R+j\omega L}} \equiv -\frac{V_-}{Z_0}. \tag{4.12}$$

where the characteristic impedance Z_0 is the ratio of the voltage to current for each of the respective traveling wave components. It can be written as

$$Z_0 = \sqrt{\frac{R+j\omega L}{j\omega C}} = \sqrt{\frac{L}{C}}\cdot\sqrt{1-j\frac{\omega_c}{\omega}}. \tag{4.13}$$

In the lossless case, where $\omega_c = 0$ or $\omega \gg \omega_c$, we have $Z_0 = \sqrt{\frac{L}{C}}$.

To determine the unknowns in Equations (4.5) and (4.6), let's consider the boundary conditions. Figure 4.2 shows a point-to-point net with source voltage $V_g(t)$ and source impedance R_s connected to its source junction, and load impedance Z_L connected to its load junction.

From Equation (4.5), define the reflection coefficient as the ratio between the forward traveling wave component and the backward traveling wave component to be

$$\Gamma(z) \equiv \frac{V_-e^{\gamma z}}{V_+e^{-\gamma z}}. \tag{4.14}$$

Figure 4.2: **Point-**

centred in the distri

The operating frequency in MCM designs is higher than the critical frequency, so we can use the high frequency approximations of the characteristic impedance $Z_0 = \sqrt{\frac{L}{C}}$, and the attenuation coefficient $\alpha = \frac{R}{2}\sqrt{\frac{C}{L}}$. Combine these two, we have $\alpha = \frac{R}{2Z_0}$. Substitute α into Equation (4.22), we have

$$H(\omega) \approx e^{-j\beta l} \frac{2e^{-\frac{Rl}{2Z_0}}}{\left[1 + \frac{R_s}{Z_0} + (1 - \frac{R_s}{Z_0})e^{-2j\beta l}e^{-2\frac{Rl}{2Z_0}}\right]}. \tag{4.23}$$

The necessary and sufficient condition for the line to be stable is $|H(\omega)| \leq 1$ at resonance. Please note that we can only optimize designs which satisfy $(1 - \frac{R_s}{Z_0}) \geq 0$. The other case where $(1 - \frac{R_s}{Z_0}) < 0$ means R_s is greater than Z_0 and already introduces too much loss. Resonance occurs approximately when $2\beta l = \pi$. So $e^{-2j\beta l} = e^{\pi j} = \cos(\pi) + j\sin(\pi) = -1$. Substitute this into Equation (4.23) and find its magnitude while taking the maximum value of $|H(\omega)| = 1$ for which the line remains stable, we have

$$|H(\omega)| = \left| \frac{2e^{-\frac{Rl}{2Z_0}}}{\left[1 + \frac{R_s}{Z_0} - (1 - \frac{R_s}{Z_0})e^{-\frac{Rl}{Z_0}}\right]} \right| \equiv 1. \tag{4.24}$$

Solving for $\frac{Rl}{Z_o}$, we have:

$$\frac{Rl}{Z_0} = 2ln\left[\frac{(1 - \frac{R_s}{Z_0})}{\sqrt{1 + \sqrt{(2 - \frac{R_s^2}{Z_0^2})}} - 1}\right]. \tag{4.25}$$

Plotting the normalized $\frac{R_s}{Z_0}$ and $\frac{Rl}{Z_0}$, the above equation is well approximated by a straight line, which is described by:

$$\frac{R_s}{Z_0} + \frac{1}{1.76} \cdot \frac{Rl}{Z_0} = 1. \tag{4.26}$$

The analytic formula (4.26) shows how the line characteristic impedance and the driver source impedance are related to produce the critical damping waveform on the receiver end, assuming $|Z_L| \gg |Z_0|$. Rearrange Equation (4.26) to reflect the dependency on line width, we have

$$l_{opt}(w) = 1.76 \cdot \frac{Z_0(w)}{R(w)}\left(1 - \frac{R_s}{Z_0(w)}\right). \tag{4.27}$$

The design method is to change the line width to find the $R(w)$ and $Z_0(w)$ producing the desired line length. This equation describes only the combined effects of source termination and distributed line resistance damping but leaves out the load termination effect for point-to-point nets.

To generalize the above analysis [FT87], we take the finite load impedance into consideration. In reality, Z_L is frequency dependent and imaginary, and for higher frequency, the assumption $|Z_L| \gg |Z_0|$ may not hold. Even so, this analytic formula in Equation

4.27 provides a very good first order model to solve the point-to-point net. It is easiest to manufacture interconnection lines with fixed metal and dielectric thicknesses, and vary only the line width. For any particular interconnection we need to know the driver impedance and the interconnection length. Then we choose an appropriate line width to obtain values of $R(w)$ and $Z_0(w)$ that will satisfy Equation (4.26) [FC91].

For finite load impedance and multi-terminal nets, a new analysis must be adapted to solve the problem. From the same transfer function (Equation (4.21)), without the assumption $|Z_L| \gg |Z_0|$, for critical damping, we have

$$|H(\omega)| = \left| \frac{2\frac{Z_L}{Z_L+Z_0} e^{-\frac{Rl}{2Z_0}}}{\left[1 + \frac{R_s}{Z_0} - (1 - \frac{R_s}{Z_0})(\frac{Z_L - Z_0}{Z_L+Z_0}) e^{-\frac{Rl}{Z_0}}\right]} \right| \equiv 1. \tag{4.28}$$

In order to compute the magnitude of $|H(\omega)|$, we want the value of $(1 - \frac{R_s}{Z_0})(\frac{Z_L - Z_0}{Z_L+Z_0})e^{-2j\beta l}$ to be real and negative. We already know $e^{-2j\beta l} = -1$ and $(1 - \frac{R_s}{Z_0}) \geq 0$. All we need to make sure is $(\frac{Z_L - Z_0}{Z_L+Z_0})$ is real and positive. Since Z_L can be a complex number, for example, a capacitive loading gives a Z_L which is imaginary, a Smith chart impedance transform is adapted here to find the equivalent impedance and length. By moving on the Smith chart d distance either toward or away from the generator, we will find a position where the distance from the generator is the multiplication of quarter-wave length. At this point, the transformed load impedance is real. The magnitude of the transformed impedance is $|Z_L|e^{\gamma d}$ or $|Z_L|e^{-\gamma d}$ depending on whether we are moving away or toward the generator. And the equivalent length of the line after transform is either $l + d$ or $l - d$. Again we can have two cases, in one case the transformed load impedance is greater than the characteristic impedance; in the other case it is less than. We can only optimize the former case since design changes are required for the later case. After we have transformed the Z_L, it can be treated as a real number and we can manipulate Equation (4.28). Solving for $\frac{Rl}{Z_o}$, we have

$$\frac{Rl}{Z_0} = 2ln \left[\frac{(1 - \frac{R_s}{Z_0})(1 - \frac{Z_0}{Z_L})}{\sqrt{1 + (1 - \frac{R_s^2}{Z_0^2})(1 - \frac{Z_0^2}{Z_L^2})} - 1} \right]. \tag{4.29}$$

Plotting the normalized $\frac{R_s}{Z_0}$, $\frac{Z_0}{Z_L}$, and $\frac{Rl}{Z_0}$ in Figure 4.3(a), the above equation is well approximated by a plane, which is described by:

$$\frac{R_s}{Z_0} + \frac{1}{1.76} \cdot \frac{Rl}{Z_0} + \frac{Z_0}{Z_L} = 1. \tag{4.30}$$

This equation holds for real and large Z_L only! It describes the combined effects of source termination, load termination, and distributed line resistance damping for point-to-point nets. In one extreme, if $R_s = Z_0$, we have $\frac{R_s}{Z_0} = 1$, the expression simplifies to the well known result of serial termination at the source junction. In the other extreme, if $|Z_0| = |Z_L|$, we have $\frac{Z_0}{Z_L} = 1$, the expression simplifies to the well known result of parallel termination at the load junction. What Equation (4.30) suggests is that if there is not enough termination either at the source junction or at the load junction, we can compensate it with the line resistance to meet the critical damping criteria, this is called the *distributed termination.*

Rearranging Equation (4.30) to reflect the dependency on line width, we have

$$l_{opt}(w) = 1.76 \cdot \frac{Z_0(w)}{R(w)} \left(1 - \frac{R_s}{Z_0(w)} - \frac{Z_0(w)}{Z_L}\right). \qquad (4.31)$$

Equation (4.27) is a special case of Equation (4.31) with $\frac{Z_0}{Z_L} \approx 0$. The optimal design approach to find the line width using Equation (4.27) can also be applied here. It is easiest to manufacture interconnection lines with fixed metal and dielectric thicknesses, and vary only the line width. For any particular interconnection we need to know the driver impedance, the load impedance, and the interconnection length. Then we choose an appropriate line width to obtain values of $R(w)$ and $Z_0(w)$ that will satisfy Equation (4.31).

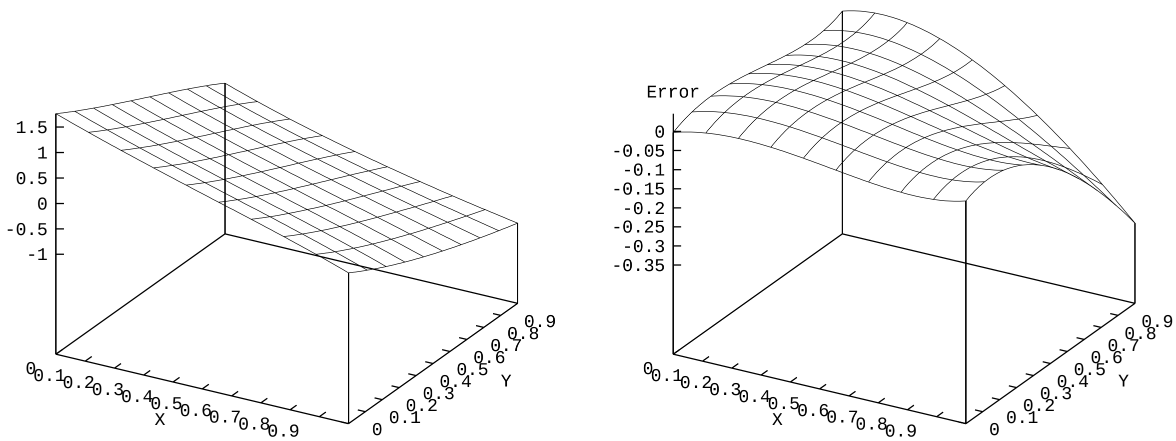

(a) (b)

Figure 4.3: **3D plot of the solution and the approximation error.** This figure shows the 3D plot of solution in (a). The x-axis is $\frac{R_s}{Z_0}$, the y-axis is $\frac{Z_0}{Z_L}$, and the z-axis is $\frac{Rl}{Z_0}$. The approximation error is plotted in (b). Because the feasible solution is only found above the x-y plane, we can ignore right half of the error plot.

Define the approximation error to be

$$error \equiv \left(\frac{\frac{Rl}{Z_0} \text{ value found with equation(4.30)}}{\frac{Rl}{Z_0} \text{ value found with equation(4.29)}} - 1\right) \times 100\%. \qquad (4.32)$$

Figure 4.3(b) shows the error introduced by this approximation. Note that the plane extending below x-y plane does not represent feasible solutions, because $\frac{Rl}{Z_0}$ cannot have a negative value. The error is small and can be ignored.

Now we have a method to find the optimal characteristic impedance and transmission line width for point-to-point nets so that it is optimally self-damped. In the next section, we want to extend this method to the optimization of the multi-terminal net with tree topology.

where the total length of the transmission line is l, the distance of the point to driver is z, and the propagation constant is γ.

In The rest of the this paper, we use the "impedance matching" to mean the magnitudes and the phases of the two impedances are the same [Lia87].

Consider the three terminal transmission line tree network in Figure 5.1 (b), from the circuit theory, we have the impedance looking toward the load end Z_f at the junction point

$$Z_f = Z_{in_b} \parallel Z_{in_c} = \frac{Z_{in_b} \cdot Z_{in_c}}{Z_{in_b} + Z_{in_c}} \tag{5.4}$$

To avoid any power reflection, the impedance looking both ways must match. This is necessary for the forward looking impedance Z_f to match the backward looking impedance Z_r to guarantee no power reflection at junction A in Figure 5.1 (b), that is

$$Z_r = Z_f = Z_{in_b} \parallel Z_{in_c}. \tag{5.5}$$

Now we analyze the output impedance Z_r looking from the load direction. Assume that the impedance of the first section of transmission line with length l_a is Z_{0_a}, the driver source impedance is Z_s, and the output impedance at any point along the first section of transmission line z distance from the driver is $Z_o(z)$. With z replacing $l - z$ and $e^{-\gamma z}$ replacing $e^{\gamma z}$, we have

$$Z_o(z) = Z_{0_a} \cdot \frac{(Z_s + Z_{0_a}) \cdot e^{\gamma z} + (Z_s - Z_{0_a}) \cdot e^{-\gamma z}}{(Z_s + Z_{0_a}) \cdot e^{\gamma z} - (Z_s - Z_{0_a}) \cdot e^{-\gamma z}} \tag{5.6}$$

Output impedance Z_r at junction A is obtained by setting $z = l_a$

$$Z_r = Z_o(l_a) = Z_{0_a} \cdot \frac{(Z_s + Z_{0_a}) \cdot e^{\gamma l_a} + (Z_s - Z_{0_a}) \cdot e^{-\gamma l_a}}{(Z_s + Z_{0_a}) \cdot e^{\gamma l_a} - (Z_s - Z_{0_a}) \cdot e^{-\gamma l_a}} \tag{5.7}$$

Next we analyze the input impedance Z_{in_b} looking from the source direction. Assume that the impedance of the second section of transmission line with length l_b is Z_{0_b}, the load impedance is Z_{L_1}, and the output impedance at any point along the second section of transmission line d distance from the load is $Z_{in}(d)$. Rearranging Equation (5.2), we have

$$Z_{in}(d) = Z_{0_b} \cdot \frac{(Z_{L_1} + Z_{0_b}) \cdot e^{\gamma d} + (Z_{L_1} - Z_{0_b}) \cdot e^{-\gamma d}}{(Z_{L_1} + Z_{0_b}) \cdot e^{\gamma d} - (Z_{L_1} - Z_{0_b}) \cdot e^{-\gamma d}} \tag{5.8}$$

Input impedance Z_{in_b} at junction A can be obtained by setting $d = l_b$

$$Z_{in_b} = Z_{in}(l_b) = Z_{0_b} \cdot \frac{(Z_{L_1} + Z_{0_b}) \cdot e^{\gamma l_b} + (Z_{L_1} - Z_{0_b}) \cdot e^{-\gamma l_b}}{(Z_{L_1} + Z_{0_b}) \cdot e^{\gamma l_b} - (Z_{L_1} - Z_{0_b}) \cdot e^{-\gamma l_b}} \tag{5.9}$$

Similarly we have the input impedance Z_{in_c} looking from the source direction.

$$Z_{in_c} = Z_{in}(l_c) = Z_{0_c} \cdot \frac{(Z_{L_2} + Z_{0_c}) \cdot e^{\gamma l_c} + (Z_{L_2} - Z_{0_c}) \cdot e^{-\gamma l_c}}{(Z_{L_2} + Z_{0_c}) \cdot e^{\gamma l_c} - (Z_{L_2} - Z_{0_c}) \cdot e^{-\gamma l_c}} \tag{5.10}$$

Substitute Equation (5.7), (5.9), and (5.10) into Equation (5.5), we have

$$\begin{aligned} Z_{0_a} \cdot \frac{(Z_s + Z_{0_a}) \cdot e^{\gamma l_a} + (Z_s - Z_{0_a}) \cdot e^{-\gamma l_a}}{(Z_s + Z_{0_a}) \cdot e^{\gamma l_a} - (Z_s - Z_{0_a}) \cdot e^{-\gamma l_a}} \quad = \quad & Z_{0_b} \cdot \frac{(Z_{L_1} + Z_{0_b}) \cdot e^{\gamma l_b} + (Z_{L_1} - Z_{0_b}) \cdot e^{-\gamma l_b}}{(Z_{L_1} + Z_{0_b}) \cdot e^{\gamma l_b} - (Z_{L_1} - Z_{0_b}) \cdot e^{-\gamma l_b}} \parallel \\ & Z_{0_c} \cdot \frac{(Z_{L_2} + Z_{0_c}) \cdot e^{\gamma l_c} + (Z_{L_2} - Z_{0_c}) \cdot e^{-\gamma l_c}}{(Z_{L_2} + Z_{0_c}) \cdot e^{\gamma l_c} - (Z_{L_2} - Z_{0_c}) \cdot e^{-\gamma l_c}} \end{aligned} \tag{5.11}$$

The known variables are $Z_s, l_a, Z_{L_1}, l_b, Z_{L_2}$, and l_c. The unknown variables are Z_{0_a}, Z_{0_b}, and Z_{0_c}.

Note that in the previous derivation, there is no information on the transfer function. The above equation holds true whether the transmission line segments are underdamped, critical damped, or overdamped. We apply the critical damping criteria because we want to optimally design self-damped lossy transmission lines. If we apply the analysis of point-to-point net to each of the branches, assuming critical damping for all, we have three more equations, which help to solve the unknown variables.

Let's focus on the branch b in Figure 5.1 (b). From previous discussion of necessary and sufficient condition for critical damping, the $\angle H(\omega)$ must equal π while Z_L and R_s is real and reasonable. So the resonant frequency is approximated by $2\beta l = \pi$, that is, $\beta l = \frac{\pi}{2}$, so

$$e^{j\beta l} = \cos(\frac{\pi}{2}) + j\sin(\frac{\pi}{2}) = j, \text{ and } \quad e^{-j\beta l} = \cos(\frac{-\pi}{2}) + j\sin(\frac{-\pi}{2}) = -j.$$

The high frequency approximation of α is $\alpha = \frac{R}{2Z_0}$, so $\alpha \cdot l = \frac{Rl}{2Z_0}$. Plug in $\gamma = \alpha + j\beta$ in Equation (5.9), we have

$$Z_{in_b} = Z_{in}(l_b) = Z_{0_b} \cdot \frac{(Z_{L_1} + Z_{0_b}) \cdot e^{\frac{Rl_b}{2Z_{0_b}}} - (Z_{L_1} - Z_{0_b}) \cdot e^{-\frac{Rl_b}{2Z_{0_b}}}}{(Z_{L_1} + Z_{0_b}) \cdot e^{\frac{Rl_b}{2Z_{0_b}}} + (Z_{L_1} - Z_{0_b}) \cdot e^{-\frac{Rl_b}{2Z_{0_b}}}}. \tag{5.12}$$

Similarly, we have

$$Z_{in_c} = Z_{in}(l_c) = Z_{0_c} \cdot \frac{(Z_{L_2} + Z_{0_c}) \cdot e^{\frac{Rl_c}{2Z_{0_c}}} - (Z_{L_2} - Z_{0_c}) \cdot e^{-\frac{Rl_c}{2Z_{0_c}}}}{(Z_{L_2} + Z_{0_c}) \cdot e^{\frac{Rl_c}{2Z_{0_c}}} + (Z_{L_2} - Z_{0_c}) \cdot e^{-\frac{Rl_c}{2Z_{0_c}}}}. \tag{5.13}$$

If the resistivity of a metal line with thickness t and width w is ρ, then the per unit length resistance of the line R is given by

$$R = \frac{\rho}{t \cdot w} \tag{5.14}$$

According to Equation (5.14), the line resistance falls inversely with increasing line width. The characteristic impedance of the line also falls inversely with increasing line width, however it does not follow a simple algebraic equation like line resistance and decreases more slower with increasing width. The values of characteristic impedance and line resistance are used to find relationships between line length and width that result in critically damped behavior for a given line dimensions. Equation (4.31) reflects the dependency of characteristic impedance and line resistance on line width.

Now we turn our attention to multi-terminal networks, their topologies can be represented as a tree. The driver is the root of the tree, the receivers are the leaves of the tree, and the junctions are the nodes of the tree. For a tree, the incoming branch of a node is defined as the branch incident to its immediate predecessor. The outgoing branch is defined as the branch incident to its immediate successor. For each node in a tree, there is only one incoming branch except for the root; and there are one or more outgoing branches except for the leaves.

In our method, we size each branch of the network by varying its width to achieve critical damped criteria. Our assumption here is that combined input impedances of the outgoing branches at the junction are also the loading impedance of the incoming branch. This is based upon the concept of "impedance matching".

other than b in the tree.
END.
FOR Each branch in the tree from leaves to root
Compute the driving point impedance of the incoming branch
of the node for which all the characteristic impedance
of the outgoing branches are known.
Find the optimal width and the characteristic impedance for
the branches with known driving point impedance
using Equation (4.31).
END.
UNTIL The widths of all branches converge.
RETURN The widths of all the branches of the tree.
END.

6 Example

To illustrate our method, we consider the two multi-terminal tree networks shown in Figure 6.1 (a) and (c). These tree network consists of one driver and many receivers. The driver is modeled by a 12Ω resistor. The loading capacitances for all receivers vary form $0.75pF$ to $1.60pF$. We present the simulation results of the initial designs which are underdamped and overdamped, together with the simulation results of critical damping obtained by using our optimal design method. The optimal design uses comparable routing resource as the overdamped cases, and far less routing resource than the underdamped cases.

Example 1: In case we use uniform width of $82\mu m$, the lines will be underdamped. On the other hand, if we use $3.4\mu m$, the lines will be overdamped. Our optimal design produces widths ranging from $3.1\mu m$ to $24\mu m$. The width of each branch is show in table 1. The simulation results are shown in Figure 6.1 (b). It shows less delay than the overdamped design and no ringing as in the underdamped design.

Table 1: Width and Length of Branches in Example 1

Branch 1	5.0mm	24.0μm
Branch 2	10.0mm	11.8μm
Branch 3	5.0mm	3.4μm
Branch 4	10.0mm	4.5μm
Branch 5	10.0mm	3.3μm
Branch 6	10.0mm	10.5μm
Branch 7	5.0mm	3.4μm
Branch 8	10.0mm	3.3μm
Branch 9	20.0mm	3.1μm

Example 2: In case we use uniform width of $82\mu m$, the lines will be underdamped. On the other hand, if we use $15\mu m$, the lines will be overdamped. Our optimal design produces widths ranging from $1.4\mu m$ to $60\mu m$. The width of each branch is show in table 2. Our optimal design method cannot optimize the first segment in this tree because the size of this tree. However, this only results in a slight overdamping on all the output waveforms. The

simulation results are shown in Figure 6.1 (d). It shows less delay than the overdamped design and no ringing as in the underdamped design.

Table 2: Width and Length of Branches in Example 2

Branch 1	12.56mm	60.0μm
Branch 2	7.55mm	34.1μm
Branch 3	2.16mm	11.0μm
Branch 4	9.41mm	8.9μm
Branch 5	0.31mm	1.1μm
Branch 6	9.68mm	6.7μm
Branch 7	0.26mm	7.0μm
Branch 8	1.08mm	1.6μm
Branch 9	7.26mm	12.9μm
Branch 10	2.20mm	2.8μm
Branch 11	9.70mm	1.1μm
Branch 12	7.57mm	1.0μm
Branch 13	7.30mm	5.2μm
Branch 14	7.55mm	1.0μm
Branch 15	2.17mm	2.9μm
Branch 16	9.70mm	1.2μm

7 Concluding Remarks

This optimal design method is to increase the line resistive losses until the fundamental resonance of the line is critically damped [FC91] [Fry92]. The frequency response is designed to fall off above this resonant frequency without any resonant peak. The basic idea is to add enough losses to damp out the reflection and resonance, but not too much to degrade the rise time and propagation delay of the high speed signal. The analysis shows for the process parameters in the example that the maximum length is about 35cm[FT87].

The other limitation comes from the critical damping criteria for branches in multi-terminal net. This imposes a limitation on the maximum length of the line. This is not a limitation in propagating high speed signal, it is a limitation on the capability to critically damp the line. Using the same process parameters for this example, if the load impedance is 214Ω at 400 MHz, and the per unit length resistance for the line is $2.4\Omega/cm$, the maximum length for the line that we can apply our optimal design method to is $10cm$. To extend the limitation, wider interconnections with lower per unit length resistance are required. Beyond this length, the response falls inversely with the square of the length becoming overdamped. This waveform has no overshoot or undershoot but suffers from longer propagation delay.

According to our optimization equation, the finite source impedance and load impedance reduces this maximum length considerably. This is not to say that this particular choice of structural and processing parameters is necessarily adequate to achieve optimum performance, instead this means that given any structural and processing parameters, our design method will find an optimal solution if it is feasible.

Due to the limited space and heat dissipation problem, the interconnections on multichip module are better left unterminated. The metal and dielectric film thickness commonly used

in the fabrication of multichip module is well suited for the design of optimal, self-damped interconnections. We have presented the analysis of point-to-point lossy transmission line leading to optimal design method for adjusting line resistance to critically damp out the reflection and resonance, taking into account both the driver source impedance and finite load impedance. We then extend this optimal design method to cover multi-terminal tree networks by decomposing each of the tree network into point-to-point segments. The result is fast and stable signal propagation for most single source multi-terminal tree topology networks up to the quarter-wavelength resonance of the line, above which the response is attenuated. For practical multichip module sizes, the bandwidth of the interconnection is more than adequate for propagating high speed digital signals for high performance systems, while eliminating the excessive heat dissipation that accompanies resistive terminations. The future research includes taking cross coupling and frequency dependent model into consideration, and verification of results through measurement.

8 Acknowledgment

This work was supported in part by the National Science Foundation Presidential Young Investigator Award under the Grant MIP-9009945, in part by Semiconductor Research Corporation under the Grant SRC-90-DJ-196, and in part by IBM Corp.

References

[BMH89] R. H. Bruce, W. P. Meuli, and J. Ho. Multichip modules. In *Proceeding of 26th Design Automation Conf.*, pages 389–393, 1989.

[Bre91] John. R. Brews. Overshoot-controlled rlc interconnections. *IEEE Trans. on Electron Device*, 38:76–87, January 1991.

[BST87] C. J. Barlett, J. M. Segelken, and N. A. Teneketges. Multichip packaging design for vlsi-based systems. *IEEE Trans. on Components, Hybrids and Manufacturing Technology*, CHMT-12(2):647–653, 1987.

[DKR+90] A. Deutsch, G. V. Kopcsay, V. A. Ranieri, J. K. Cataldo, E. A. Galligan, W. S. Graham, R. P. McGouey, S. L. Nunes, J. R. Paraszczak, J. J. Ritsko, R. J. Serino, D. Y. Shih, and J. S. Wilczynski. High-speed signal propagation on lossy transmission lines. *IBM J. Res. Develop*, 34(4):601–615, July 1990.

[FC91] Robert C. Frye and Howard Z. Chen. High speed interconnection using self-damped lossy transmission lines. In *Symposium on High Density Integration in Comunication and Computer Systems*, pages 36–37, 1991.

[Fry92] Robert C. Frye. Private communication. 1992.

[FT87] R. C. Frye and K. L. Tai. Interconnection lines for wafer-scale-integrated assemblies. *U. S. Patent 4,703,288*, 1987.

[HCBA82] C. W. Ho, D. A. Chance, C. H. Bajorek, and R. E. Acosta. The thin-film module as a high performance semiconductor package. *IBM Journal Res. Develop*, 26(286), 1982.

[Lia87] Simuel Y. Liao. *Microwave Circuit Analysis and Amplifier Design.* Prentice-Hall, Inc., 1987.

[Ohs89] Takaaki Ohsaki. VLSI packaging technologies for high speed electronic systems. In *Proceeding of VLSI 89*, pages 255–264, 1989.